Orbital current and torque at the interface of magnetic tunnel junctions

Jun-ichiro Inoue,[1,*] Masahito Tsujikawa,[1] and Masafumi Shirai[1,2]
[1]*Research Institute of Electrical Communication, Tohoku University, Sendai 980-8577, Japan*
[2]*Center for Science and Innovation in Spintronics (CSIS), Core Research Cluster (CRC), Tohoku University, Sendai 980-8577, Japan*

(Received 27 February 2023; revised 20 May 2023; accepted 13 July 2023; published 27 July 2023)

This study formulated the longitudinal spin and orbital currents and torques in the nonequilibrium Green's function formalism for magnetic tunnel junctions with spin-orbit coupling (SOC). The analytical results for the y and z components of the spin currents without SOC are consistent with those previously reported. We show that the torque induced by the SOC is transmitted through the junction, resulting in an orbital coupling between the two magnetic layers. Orbital torque deduced from the analytical expressions exhibits several unique features. Orbital mixing is crucial to the orbital torque, and the torque may remain finite even for nonmagnetic-ferromagnetic tunnel junctions. The result was interpreted in terms of long-range character of the magnetic anisotropy and nondegeneracy of orbital states. The effects of finite voltage applied to the junctions have also been clarified.

DOI: 10.1103/PhysRevB.108.014431

I. INTRODUCTION

The field of spintronics emerged from the discovery of the giant and tunnel magnetoresistance [1,2], which facilitates control of the charge current via spin. Successively, methods of spin control by charge current, which utilize spin-injection, spin-transfer torque, etc., have been proposed [3,4]. In these phenomena, the spin-polarized longitudinal currents play an essential role. Subsequently, transverse current of spins without a charge current, that is, the spin Hall effect (SHE), was proposed for a two-dimensional electron gas with spin-orbit coupling (SOC) [5–7]. In the SHE, up- and down-spin electrons, that is, the z components of the spin angular momentum (SAM), flow in opposite directions. Moreover, the flow may produce spin accumulation at the edges of samples [8,9]. Thus, it was proposed that the SHE is effective for spin injection to realize control of the magnetization direction of thin films in metallic layered systems [10,11]. Additionally, it was reported that SOC is crucial for converting the spin polarization of the current to the SAM in adjacent films [12,13]. Furthermore, numerical calculations of SHE performed for transition metals indicated that a large SHE occurs in realistic transition metals [14–16].

Kontani *et al.* [14–16] predicted that transverse current of the orbital angular momentum (OAM), referred to as orbital Hall effect (OHE), may occur in transition metals. The most intriguing point is that a large OHE exists in nonmagnetic metals (NMs) with no SOC. The origin of this effect has been interpreted in terms of momentum-space magnetic field, that is, Berry curvature [17]. Because of the similarity between the SHE and OHE, the orbital-spin conversion [18,19], orbital torque caused by OHE [20,21], and orbital Edelstein effect [22] have been proposed. The intrinsic OHE has been predicted to appear also in two-dimensional transition metal dichalcogenides [23] and group XIV materials [24]. In addition, observations of orbital torque have been reported [25].

Another important concept in spintronics is interlayer coupling of spin moments in magnetic junctions, where two ferromagnetic metal (FM) layers are separated by a thin NM layer [26–29]. Experiments have reported that the magnetic coupling oscillates as a function of NM layer thickness. The phenomenon was formulated in terms of the interlayer current of the y component of spin, in contrast to the z component of spin (the direction of magnetic moment). The basic formula is expressed in terms of the nonequilibrium (Keldysh) Green's function (GF) [30,31]. However, the final expression is presented using the ordinary perturbation method because the interlayer coupling itself is a phenomenon occurring in the equilibrium state [32]. The numerical results were consistent with experimental observations [33,34]. Considering the aforementioned situations for the SHE, OHE, and the longitudinal spin current, it is expected that an orbital current, that is, the longitudinal current of OAM, may also exist at magnetic junctions.

The longitudinal spin current in magnetic junctions is different from the transverse spin current in SHE. The transverse current of the Hall conductivity has been calculated in the linear response theory, and it vanishes in the zero-bias limit. On the other hand, the longitudinal spin current through a junction has been defined as the time variation of the relative angle of SAMs on the ferromagnetic layers in magnetic junctions, and therefore it vanishes in the magnetically stable (equilibrium) state. When the SAM of one FM layer of the junction rotates from the stable state, there appears a torque to restore the unstable state, and the spin current at the junction becomes finite at the junction. The torque is called spin torque [32]. Thus the spin current exists even in the zero-bias limit. In a similar way, orbital torque could be defined as the time

*inoue.junichiro.u5@a.mail.nagoya-u.ac.jp

variation of OAM in ferromagnetic junctions. It is noted that existence of magnetic moment is indispensable, and no spin and orbital torques exist in paramagnetic junctions. The concept of the orbital torque is thus different from that introduced in Ref. [20]. Mathematically, the time derivative of the spin moment, that is, the spin current, is expressed by using the nonequilibrium GF, and the expression itself includes effects of finite-bias states as well as those in the zero-bias state.

The aim of this paper is to clarify the characteristics of the longitudinal spin and orbital currents through a tunneling barrier in magnetic junctions with SOC. To this end, we derive analytical expressions of the longitudinal spin and orbital currents adopting simple models and a second-order approximation. Inclusion of SOC is essential for the longitudinal orbital current/torque, because the OAM is induced via SOC in ferromagnetic metals and strongly coupled with the spin state. In the approximation, however, we assume collinear alignment of SAM and OAM, and neglect the change in the spin and orbital states of each FM layer when they rotate. The rotation may be called uniform rotation. The effects of finite bias voltage on the spin and orbital currents will be also investigated.

We demonstrate that an orbital current exists and produces an orbital torque that acts between the two canted magnetic moments of the FM layers. Interestingly the torque can be nonzero even when one of the metals is nonmagnetic. The existence of the orbital torque is interpreted in terms of the long-range character of the magnetic anisotropy (MA) induced by the SOC and nondegeneracy of orbital states. In addition, we show that SOC produces an additional dependence of the spin and orbital torques on the angle between the two canted magnetic moments. Finally, we estimate the magnitude of orbital coupling, with a discussion of the magnitude of orbital moments near the MgO/Fe interface [35]. Furthermore, possible methods for observing the orbital coupling are discussed. The results would be useful for interpretation of results in future experiments.

The remainder of this paper is organized as follows. Section II describes the basic formula for the spin and orbital currents, the simplified model and Hamiltonian, and approximations to treat the nonequilibrium GF and SOC. The analytical results of spin current/torque and orbital current/torque are provided in Sec. III. In the same section, we also give discussions on the model and approximations and estimate magnitude of the orbital torque in ferromagnetic tunnel junctions. The summary of the work is presented in the final section.

II. MODEL AND FORMALISM

A. Spin and orbital currents

The time derivative of physical quantity $\boldsymbol{F}$ is given by the Heisenberg equation, $d\boldsymbol{F}/dt = (i/\hbar)[H, \boldsymbol{F}]$, where H denotes Hamiltonian. When quantity $\boldsymbol{F}$ is considered a local quantity at site m, $d\boldsymbol{F}_m/dt$ is the divergence of the quantity at site m, that is, the difference between incoming and outgoing quantities. When $\boldsymbol{F}_m$ is the charge, spin, or orbital density at site m, $d\boldsymbol{F}_m/dt$ may yield the corresponding current depending on the Hamiltonian in the equation.

Thus, the charge current at site m is expressed as $d\boldsymbol{n}_m/dt$ for the Hamiltonian with nearest-neighbor hopping. In this case, the expectation value includes terms such as $\langle a^\dagger_{m\mu\sigma} a_{nv,\sigma'}\rangle$, which may be expressed in terms of the nonequilibrium GF, defined as [32,36]

$$G^+_{nv\sigma',m\mu\sigma}(t, t^+) \equiv \frac{i}{\hbar}\langle a^\dagger_{m\mu\sigma}(t^+) a_{nv\sigma'}(t)\rangle. \tag{1}$$

In the limit of $t' \to t$, and after Fourier transformation into ω space, the electric charge current at site m is expressed as

$$\langle J^C_m\rangle = \frac{e}{2\pi\hbar}\mathrm{Tr}_{(\mathrm{spin,orb})}\int d\omega(\boldsymbol{A}_{mm\uparrow\uparrow} + \boldsymbol{A}_{mm\downarrow\downarrow}), \tag{2}$$

with

$$\boldsymbol{A}_{mm} = \boldsymbol{G}^+_{mn}\boldsymbol{t}_{nm} - \boldsymbol{t}_{mn}\boldsymbol{G}^+_{nm}, \tag{3}$$

where $\boldsymbol{t}_{mn}$ indicates the hopping Hamiltonian between the sites m and n, and $\boldsymbol{A}_{mm}$ is a matrix for both spin and orbital spaces.

Because of the charge conservation law, the expression Eq. (2) is apparent. However, the spin and orbital currents are not necessarily conserved when the directions of SAM and OAM vary spatially. In the following, we consider the electron hopping through a tunnel barrier as a source of spin and orbital currents in magnetic tunnel junctions, because we are interested in the torque caused by the relative rotation of magnetic moments on magnetic layers in the junction. Other sources of spin and orbital currents/torques are neglected. We also consider change in the electronic states due to SOC near the junction interface, since it may modify the electron hopping through the tunnel barrier. Here, change in the spin and orbital moments is not included. The situation may correspond to the uniform rotation of the magnetic moment in each magnetic layer; that is, the rotation satisfies the collinearity and no change in magnitude of spin and orbital moments. In a simple one-dimensional model explained below, the time derivative of SAM and OAM at a single site may provide sufficient information on the spin and orbital currents through the barrier interface.

Mathematically, we adopt the following approximations to calculate the time variation of SAM and OAM. We consider only the hopping Hamiltonian at the tunnel barrier for $\boldsymbol{H}$ in the Heisenberg equation. Although the SOC is ignored for $\boldsymbol{H}$ in the Heisenberg equation, it is included in the definition of the Green's function $\boldsymbol{G}^+_{mn}$ to treat the change in the electronic states produced by the uniform rotation. Effects of spin mixing in the electron hopping at the junction barrier are also considered.

After these approximations, the spin and orbital currents at site m are expressed as before,

$$\langle \boldsymbol{J}^S_m\rangle = \frac{1}{4\pi}\mathrm{Tr}_{(\mathrm{orb})}\int d\omega \boldsymbol{A}_{mm}\boldsymbol{\sigma}, \tag{4}$$

$$\langle \boldsymbol{J}^L_m\rangle = \frac{1}{2\pi}\mathrm{Tr}_{(\mathrm{spin})}\int d\omega \boldsymbol{A}_{mm}\boldsymbol{L}/\hbar, \tag{5}$$

respectively. Here, $\boldsymbol{\sigma}$ and $\boldsymbol{L}$ are Pauli spin matrix and OAM matrix, respectively, and the operators $\boldsymbol{\sigma}$ and $\boldsymbol{L}/\hbar$ play a role of projection of $\boldsymbol{A}_{mm}$ onto the spin and orbital spaces, respectively. As can be seen from the definition of $\boldsymbol{A}_{mm}$ in Eq. (3), the

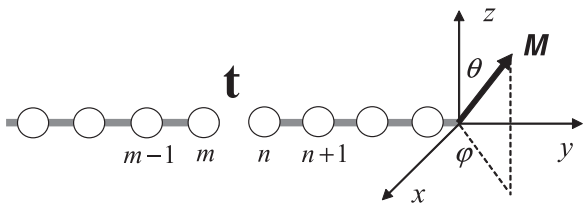

FIG. 1. Schematic figure of one-dimensional lattice, which is divided into three parts: left part including sites m, $m-1$, etc.; right part with sites n, $n+1$, etc.; and an insulator region between sites m and n with hopping Hamiltonian $\boldsymbol{t}$. Sites m and n are edge sites of the left and right parts of electrodes. The direction of magnetic moment $\boldsymbol{M}$ on right part is canted by an angle (θ, φ) with respect to that on left part (not shown) parallel to z axis as shown in the figure.

currents given by Eqs. (4) and (5) are those that flow through a junction interface.

Torque is defined as follows [32,36]. When the quantity $\boldsymbol{F}_m$ is an angular momentum (AM), the time derivative of $\boldsymbol{F}_m$ denotes the torque acting on AM. Then, the explicit expression of $d\boldsymbol{F}_m/dt$ for SAM and OAM at site m must yield spin and orbital torques, respectively. Because the torque is caused by a relative rotation of AMs on the left and right lattices, no torque is exerted on the whole system. The torque we are interested in is a relative torque appearing at the junction interface, and is given by the difference in the spin or orbital currents at sites m and n, which are located at the edges of the two metallic electrodes (see Fig. 1). For example, the y component of the relative torque acting at the junction is expressed as

$$N_{mn}^{Sy(Ly)}(\theta) = \langle J_m^{Sy(Ly)} \rangle - \langle J_n^{Sy(Ly)} \rangle, \tag{6}$$

for $\varphi = 0$. It is noted that $\langle J_m^{Sy(Ly)} \rangle$ is opposite in sign to $\langle J_n^{Sy(Ly)} \rangle$, which has been confirmed by analytical expressions obtained.

When the direction of the SAM (or OAM) on the left electrode is different from that on right electrode by the angle θ, coupling energy $E(\theta) = \tilde{J}\cos\theta$ is produced. This energy is related to torque by $N(\theta) = dE(\theta)/d\theta$ [32,36]. Thus, the coupling constant $E(0)$ can be evaluated. We formulate spin and orbital currents and relative torques at the interface using Eqs. (3)–(5), and clarify their characteristics. In the following, we call the relative torque $\boldsymbol{N}_{mn}$ simply torque at the junction, since it relates to the coupling of SAM (OAM) on left and right lattices.

B. Model Hamiltonian

We consider tunnel junctions in which two magnetic metals are separated by a thin insulating layer. The lattice of the junction exhibits a cubic symmetry, and the electronic structure is presented in a tight-binding Hamiltonian as follows:

$$H = H_T + H_{\rm ex} + H_{\rm SOC}, \tag{7}$$

$$H_T = \sum_{i,j,\sigma,\sigma'} \sum_{\mu,\nu} t_{ij\sigma\sigma'}^{\mu\nu} a_{i\mu\sigma}^\dagger a_{j\nu\sigma'}, \tag{8}$$

where $t_{ij\sigma\sigma'}^{\mu\nu}$ indicates electron-hopping between the nearest-neighbor sites i and j, and indices (σ, μ) and (σ', ν) are the spin and orbital at sites i and j, respectively. Wave functions can be expressed using mixed representation with a wave number parallel to the junction plane and layer indices perpendicular to junction plane. However, in practice, we adopt a one-dimensional lattice model, as shown in Fig. 1, to render analytical study feasible. In addition, we use the t_{2g} model, wherein xy, yz, and zx orbitals are included, because the essence of the orbital properties is maintained in the model. The Hamiltonian $H_{\rm ex}$ denotes the on-site exchange potential treated in the Hartree-Fock approximation. As a result $H_{\rm ex}$ is expressed as on-site, spin-dependent energy levels. $H_{\rm SOC}$ denotes the SOC, given practically by the on-site L-S coupling,

$$\hbar\xi[(\sigma_+ L_- + \sigma_- L_+)/2 + \sigma_z L_z] \equiv \boldsymbol{V}, \tag{9}$$

where ξ denotes the coupling energy. Thus, H is easily manipulated as a tight-binding Hamiltonian.

We define the charge, spin, and orbital currents as time derivatives of the charge, spin, and orbital densities, respectively, at site i, expressed as

$$\boldsymbol{n}_i = \sum_{\mu\sigma} a_{i\mu\sigma}^\dagger a_{i\mu\sigma}, \tag{10}$$

$$\boldsymbol{s}_i = \frac{\hbar}{2} \sum_{\mu} (a_{i\mu\uparrow}^\dagger \quad a_{i\mu\downarrow}^\dagger) \boldsymbol{\sigma} \begin{pmatrix} a_{i\mu\uparrow} \\ a_{i\mu\downarrow} \end{pmatrix}, \tag{11}$$

$$\boldsymbol{l}_i = \sum_{\sigma} (a_{i1\sigma}^\dagger \quad a_{i2\sigma}^\dagger \quad a_{i3\sigma}^\dagger) \boldsymbol{L} \begin{pmatrix} a_{i1\sigma} \\ a_{i2\sigma} \\ a_{i3\sigma} \end{pmatrix}, \tag{12}$$

respectively. Here, $\boldsymbol{L}$ is defined as

$$L_x/\hbar = \begin{bmatrix} 0 & 0 & -i \\ 0 & 0 & 0 \\ i & 0 & 0 \end{bmatrix}, \quad L_y/\hbar = \begin{bmatrix} 0 & i & 0 \\ -i & 0 & 0 \\ 0 & 0 & 0 \end{bmatrix},$$
$$L_z/\hbar = \begin{bmatrix} 0 & 0 & 0 \\ 0 & 0 & i \\ 0 & -i & 0 \end{bmatrix}, \tag{13}$$

for the t_{2g} model. Indices 1, 2, and 3 denote the xy, yz, and zx orbitals, respectively. Here the x, y, and z axes are defined as shown in Fig. 1, and up ($\uparrow$) and down ($\downarrow$) spins are the z components of SAM.

Now, we specify the practical form of H_T corresponding to the one-dimensional model shown in Fig. 1. H_T is divided into the following three parts: the left (L) and right (R) parts and an insulator part. The matrix forms of the hopping terms are assumed to be

$$\boldsymbol{H}_T^L = \boldsymbol{H}_T^R = \begin{bmatrix} h_1 & 0 & 0 \\ 0 & h_2 & 0 \\ 0 & 0 & h_3 \end{bmatrix}, \tag{14}$$

$$\boldsymbol{t}_{mn} = \mathbf{t}_{nm} = \begin{bmatrix} t_1 & 0 & 0 \\ 0 & t_2 & 0 \\ 0 & 0 & t_3 \end{bmatrix}, \tag{15}$$

respectively, in the order of the xy, yz, and zx orbitals. Here, $h_1 = h_2 \neq h_3$ for the model shown in Fig. 1. As evident, the present model can easily be generalized to a three-dimensional model with a simple cubic lattice, by introducing an in-plane wave vector, defined on the junction interface. When the magnetic moment on the R lattice is canted to that of the L lattice at an angle (θ, φ), as shown in Fig. 1, the hopping

Hamiltonian $\boldsymbol{t}_{mn}$ depends on the angles θ and φ. However, in practice, $\varphi = 0$ is often used for simplicity.

C. Approximations to nonequilibrium GF

As we focus our study on a tunnel junction in which a thin insulating barrier is inserted between the two metals, the tunneling Hamiltonian $\boldsymbol{t}_{mn}$ can be treated as a second-order perturbation. When $\boldsymbol{t}_{mn} = 0$, the two metals are in equilibrium, and their GFs are denoted by $\boldsymbol{g}^{A(R)}$ and $\boldsymbol{g}^{+(-)}$, respectively. The perturbation method for nonequilibrium states is nonconventional. Herein, we used the methods proposed by Caroli *et al.* [30,31], which provide well-known results of Bardeen's expression for the tunneling conductance.

The nonequilibrium GF formalism includes four GFs: $\boldsymbol{G}^{A(R)}$ and $\boldsymbol{G}^{+(-)}$, where $\boldsymbol{G}^{A}$ and $\boldsymbol{G}^{R}$ are the advanced and retarded GF, respectively, and $\boldsymbol{G}^{+}$ and $\boldsymbol{G}^{-}$ correspond to occupied and unoccupied states, respectively. Among these four GFs, only three are independent because the general relation $\boldsymbol{G}^{+} - \boldsymbol{G}^{-} = \boldsymbol{G}^{A} - \boldsymbol{G}^{R}$ holds, by definition.

The basic method for the second-order perturbation of the hopping integral $\boldsymbol{t}_{mn}$ in a nonequilibrium state is given by Caroli's method,

$$\begin{aligned}\boldsymbol{G}^{+}_{mn} &= \boldsymbol{g}^{R}_{mm}\boldsymbol{t}_{mn}\boldsymbol{G}^{+}_{nn} + \boldsymbol{g}^{+}_{mm}\boldsymbol{t}_{mn}\boldsymbol{G}^{A}_{nn} \\ &\simeq \boldsymbol{g}^{R}_{mm}\boldsymbol{t}_{mn}\boldsymbol{g}^{+}_{nn} + \boldsymbol{g}^{+}_{mm}\boldsymbol{t}_{mn}\boldsymbol{g}^{A}_{nn},\end{aligned} \tag{16}$$

and a similar approximation to $\boldsymbol{G}^{+}_{nm}$. In the second part of Eq. (16), $\boldsymbol{G}^{+(A)}_{nn}$ is replaced with $\boldsymbol{g}^{+(A)}_{nn}$. The general expressions for the currents include only second-order terms of $\boldsymbol{t}_{mn}$, and after straightforward computation, we obtain analytical expressions by using the general relationship $\boldsymbol{g}^{+}(\omega) - \boldsymbol{g}^{-}(\omega) = \boldsymbol{g}^{A}(\omega) - \boldsymbol{g}^{R}(\omega)$, where $g^{+}(\omega)$ and $g^{-}(\omega)$ represent the occupied and unoccupied states in the equilibrium state, and the definition of the Green's function $\boldsymbol{g}^{A(R)}(\omega)$ is

$$g^{R(A)} = P(\omega - H)^{-1} - (+)i\pi\delta(\omega - H). \tag{17}$$

D. Spin-orbit coupling

Inclusion of SOC in the formalism is crucial, for several reasons. SOC induces orbital moments that are typically quenched in metals without SOC. SOC produces MA in FMs through which the stable direction of the magnetic moment can be determined. When the direction of the magnetic moment deviates from the stable state, torque is induced to recover the stable direction. When the relative direction of magnetic moments in adjacent layers of a junction is altered, a torque may act between the magnetic moments on the two FM layers via the SOC. Moreover, new tunneling paths can be opened by mixing $\uparrow$ and $\downarrow$ spin states by the SOC, which affect both spin and orbital currents.

Despite the importance of SOC, we adopt a simplified treatment of the SOC to derive analytical expressions: the *L*-*S* coupling is introduced only at the interface of the junction, the *n*th site at the edge of the ferromagnetic *R* lattice in the present one-dimensional model, and it is treated as a second-order perturbation [37],

$$(\boldsymbol{g}_n)_{\sigma\sigma'} = \left(\boldsymbol{g}^{0}_{n} + \boldsymbol{g}^{0}_{n}\boldsymbol{V}_{n}\boldsymbol{g}^{0}_{n}\boldsymbol{V}_{n}\boldsymbol{g}^{0}_{n}\right)_{\sigma\sigma'}, \tag{18}$$

where $\boldsymbol{V}_n$ is the *L*-*S* coupling at site n and $\boldsymbol{g}^{0}_{n}$ denotes the unperturbed GF defined by using H_T and $H_{\rm ex}$. The first-order term for $\boldsymbol{V}_n$ vanishes by symmetry argument [38], and the second term includes the coupling of spin and orbital degrees of freedom. The unperturbed GF $\boldsymbol{g}^{0}_{n}$ is easily obtained in the form of a continued fraction for one-dimensional lattices [39]. Thus, $\boldsymbol{g}_m$ is a diagonal matrix in the spin and orbital space, whereas $\boldsymbol{g}_n$ includes off-diagonal elements.

Here we remark on MA of the system. The easy axis of magnetic moment in the present model is arbitrary. Although it is easily determined in the three-dimensional lattices, asymmetry in the one-dimensional lattice appears only between the y direction and z-x plane, as shown in Fig. 1. Nevertheless, we assume that the magnetic moments on the two FMs are parallel to the z axis in the stable state, and calculate the spin and orbital currents after canting the magnetic moment on the R lattice at a certain angle (θ, φ). Notably, additional effects may appear in spin (orbital) current when SOC is included in the L lattice, even if no canting of magnetic moments occurs in the L lattice.

III. ANALYTICAL RESULTS AND DISCUSSION

In this section, we present the analytical results for the z component of the spin currents, the y component of the spin torque, three components of the orbital torque in a spinless model, and the y component of the orbital torque including the spin degrees of freedom. We omitted results for the x components of spin and orbital torques except for the result given in Eq. (23), because their essential features are the same as those of the y component.

A. Spin current and torque

Here, we formulate explicit expressions for the z component of the spin current and y component of the spin torque using Eqs. (4) and (6). Orbital degrees of freedom were included by taking traces over the orbitals.

First, we show the expression for the z component of the spin current, which is the difference between the up- and down-spin currents under finite voltage. The expression obtained for $\varphi = 0$ is

$$\begin{aligned}\langle J^{Sz}\rangle = \pi \sum_{\mu} t_{\mu}^{2} \int d\omega [&F_1 \cos^2(\theta/2) + F_2 \sin^2(\theta/2) \\ &+ F_3 \sin(\theta/2)][f_L(\omega) - f_R(\omega)],\end{aligned} \tag{19}$$

where

$$\begin{aligned}F_1 &= D_{L\uparrow\mu}(\omega)D_{R\uparrow\uparrow\mu}(\omega) - D_{L\downarrow\mu}(\omega)D_{R\downarrow\downarrow\mu}(\omega), \\ F_2 &= D_{L\uparrow\mu}(\omega)D_{R\downarrow\downarrow\mu}(\omega) - D_{L\downarrow\mu}(\omega)D_{R\uparrow\uparrow\mu}(\omega), \\ F_3 &= [D_{L\uparrow\mu}(\omega) + D_{L\downarrow\mu}(\omega)][D_{R\uparrow\downarrow\mu}(\omega) + D_{R\downarrow\uparrow\mu}(\omega)].\end{aligned}$$

Here, $f_{L(R)}(\omega)$ is the Fermi distribution function of the L (R) lattice, and $D_{L\sigma\mu}(\omega)$ and $D_{R\sigma\sigma'\mu}(\omega)$ are the imaginary parts of $g^{L}_{mm\sigma\mu}(\omega)$ and $g^{R}_{nn\sigma\sigma'\mu}(\omega)$, respectively, which are orbital diagonals because $\boldsymbol{g}^{R}_{mm}$ and $\boldsymbol{t}_{mn}$ are orbital diagonals, even though $\boldsymbol{g}^{R}_{nn}$ includes effects of the SOC.

F_1 and F_2 are ordinary spin-mixing terms in the tunneling current caused by canting of the SAM. When $\theta = 0$, the

difference between the up- and down-spin currents can be observed, as is already known. The F_3 term originates from spin mixing in the local GF of the nth site owing to SOC. Further, another angle dependence is implicitly included in $D_{R\sigma\sigma'\mu}(\omega)$ due to SOC: $\sin(2\theta)$ for $\sigma = \sigma'$, and both $\cos^2\theta$ and $\sin^2\theta$ for $\sigma \neq \sigma'$.

Next, we show the y component of the spin torque acting between SAMs on the mth and nth sites. The explicit expression of the torque defined by Eq. (6) is given as

$$N^{Sy}_{mn} = \frac{1}{\pi}\sum_{\mu} t_\mu^2 \int d\omega \{[\mathrm{Im}\, G_1\, \mathrm{Re}\, G_2 f_L(\omega) + \mathrm{Re}\, G_1\, \mathrm{Im}\, G_2 f_R(\omega)]\sin\theta + 2[\mathrm{Im}\, G_1\, \mathrm{Re}\, G_3 f_L(\omega) + \mathrm{Re}\, G_1\, \mathrm{Im}\, G_3 f_R(\omega)]\cos\theta\}, \quad (20)$$

with

$$G_1 = g^L_{m\uparrow\mu}(\omega) - g^L_{m\downarrow\mu}(\omega),$$
$$G_2 = g^R_{n\uparrow\uparrow\mu\mu}(\omega) - g^R_{n\downarrow\downarrow\mu\mu}(\omega),$$
$$G_3 = g^R_{n\uparrow\downarrow\mu\mu}(\omega) = g^R_{n\downarrow\uparrow\mu\mu}(\omega).$$

In this expression, $\sin\theta$ denotes the ordinary interlayer coupling, which vanishes for $\theta = 0$ and π, whereas the $\cos\theta$ term is a new coupling path that appears via the SOC. Additional angle dependence also appears via $g^R_{n\sigma\sigma'\mu\mu}(\omega)$ as mentioned in the case of $\langle J^{Sz}\rangle$. We note that the term G_3 includes $\sin\theta$ owing to the SOC and vanishes at $\theta \to 0$.

In the equilibrium state, the expression is reduced to

$$N^{Sy}_{mn} = \frac{1}{\pi}\sum_{\mu} t_\mu^2 \int d\omega\, \mathrm{Im}[G_1(G_2\sin\theta + 2G_3\cos\theta)]f(\omega). \quad (21)$$

The result without the G_3 term is consistent with the expression presented by Edwards *et al.* [32] in the lowest-order approximation of the interlayer hopping $\boldsymbol{t}$. Thus, in this formalism, we find that the results in a nonequilibrium state can be obtained by a replacement

$$\mathrm{Im}[G_1 G_2]f \Longrightarrow (\mathrm{Im}\, G_1\, \mathrm{Re}\, G_2)f_L + (\mathrm{Re}\, G_1\, \mathrm{Im}\, G_2)f_R \quad (22)$$

in an equilibrium state.

B. Orbital current and torque

When the directions of magnetic moments of the R and L lattices are canted by an angle (θ, φ), an orbital current may appear. Consequently, torque is induced to restore the direction of OAM. Here, we formulate the orbital current and torque acting on the OAM through the insulating layer in the junction by evaluating Eq. (6). SOC exists only at the nth site, as assumed.

First, we present the results of the orbital torque without a spin degree of freedom. In other words, we formulate an orbital current through the junction in a model with spin-independent hopping and three orbitals that are independent of the canting of OAM. The SOC, however, exists on the nth site, and the magnetic moment on the R lattice is canted by an angle (θ, φ). The model is physically fictitious; however, this may simplify the analysis and reveal the orbital and angle dependencies of the orbital torque.

The expressions obtained for the torque in the equilibrium state are expressed as

$$\boldsymbol{N}^{Lx}_{mn} = \frac{1}{\pi}\int d\omega\, \mathrm{Im}(H_{13})f \propto (\hbar\xi)^2 \sin 2\theta \sin\varphi, \quad (23)$$

$$\boldsymbol{N}^{Ly}_{mn} = -\frac{1}{\pi}\int d\omega\, \mathrm{Im}(H_{12})f \propto (\hbar\xi)^2 \sin 2\theta \cos\varphi, \quad (24)$$

$$\boldsymbol{N}^{Lz}_{mn} = -\frac{1}{\pi}\int d\omega\, \mathrm{Im}(H_{32})f \propto (\hbar\xi)^2 \sin^2\theta \sin 2\varphi, \quad (25)$$

with

$$H_{pq} = g^R_{npq}\left\{g^L_{mpp}\left(t_p t_q + t_p^2\right) - g^L_{mqq}\left(t_p t_q + t_q^2\right)\right\}, \quad (26)$$

where ξ denotes the magnitude of the SOC and p and q are the orbital indices 1,2, or 3.

The expression of Eq. (26) shows that the orbital torque depends on the electronic state of the nth and mth sites and on the orbital components of the electron hopping t_p, etc., at the junction. The results suggest that the orbital torque vanishes under the orbital degeneracy, that is, $g^L_{mpp} = g^L_{mqq}$ and $t_p = t_q$. Actually, $\boldsymbol{N}^{Ly}_{mn} = 0$ for the model given in Fig. 1. Inclusion of additional interorbital hopping at the junction, however, produces more complex expressions of the orbital torque (not shown). Thus, the existence of nondegenerate orbital states seem to be indispensable for orbital torque.

The (θ, φ) dependence of the orbital torque shown in Eqs. (23)–(25) seems to be obvious. For example, $\theta = \pi/2$ in (25) gives the maximal torque around the z axis with fixed φ, and $\varphi = 0(\pi/2)$ gives a maximal torque around $y(x)$ axis with fixed θ.

The orbital torque acting on OAM is proportional to $\boldsymbol{t}^2$ and to ξ^2. This result is also obvious because these quantities were treated in the second-order perturbation. Nevertheless, the presence of an orbital torque may require a suitable interpretation because there is no SOC and no OAM might appear in L lattice. The most likely explanation is that the torque is caused by MA induced by the existence of the junction structure. The interpretation may be supported by the long-range character of MA [38] and nondegenerate orbital states near the junction.

Next, we show the expression for the y component of the orbital torque, including spin degrees of freedom. Here, we assume that $t_1 = t_2 \equiv t$, because t_3 was found to be irrelevant in this case. The expression of the y component of the orbital torque in the equilibrium state is given as

$$\boldsymbol{N}^{Ly}_{mn} = \frac{2}{\pi}t^2 \int d\omega [\mathrm{Im}(G_m G_n)\sin\theta + 2\,\mathrm{Im}(G_{m\uparrow}G_{n\uparrow} + G_{m\downarrow}G_{n\downarrow})\cos^2(\theta/2) + 2\,\mathrm{Im}(G_{m\uparrow}G_{n\downarrow} + G_{m\downarrow}G_{n\uparrow})\sin^2(\theta/2)]f(\omega), \quad (27)$$

with

$$G_m(\omega) = G_{m\downarrow}(\omega) - G_{m\uparrow}(\omega), \quad (28)$$

$$G_n(\omega) = g^R_{nn\uparrow\downarrow 21}(\omega) + g^R_{nn\downarrow\uparrow 21}(\omega), \quad (29)$$

$$G_{m\sigma}(\omega) = g^L_{mm\sigma 2}(\omega) - g^L_{mm\sigma 1}(\omega), \quad (30)$$

$$G_{n\sigma}(\omega) = g^R_{nn\sigma\sigma 21}(\omega). \quad (31)$$

Because orbital states $1(xy)$ and $2(yz)$ are degenerate for a one-dimensional lattice with a straight line, $G_{m\sigma}(\omega)$ should vanish. Nevertheless, we retained this term in Eq. (27) for later discussion of more realistic systems.

The angular dependence of $\sin\theta$ in Eq. (27) originates from spin mixing due to the canted SAM, similar to the spin torque expressed in Eq. (21). However, it vanishes without the SOC because $G_n(\omega)$ is a term caused by SOC, as shown in Eq. (29). The terms with $\cos^2(\theta/2)$ and $\sin^2(\theta/2)$ result from the SOC included in $G_{n\sigma}(\omega)$; therefore, they also vanish as the SOC tends to zero. When $\theta = 0$, the $\cos^2(\theta/2)$ term vanishes because $g^R_{nn\sigma\sigma 21} \propto \sin 2\theta$.

Thus, the orbital torque expressed by Eq. (27) is proportional to $t^2\xi^2$ similar to that in Eq. (24). The nondegeneracy of the orbitals on the mth site is also crucial for these terms, as shown in Eq. (30). The expression for nonequilibrium states can be obtained using the procedure expressed in Eq. (22).

When the left lattice (mth site) is nonmagnetic, $g^L_{mm\uparrow 1(2)} = g^L_{mm\downarrow 1(2)} \equiv g^L_{mm01(2)}$, etc., we obtain

$$\boldsymbol{N}^{Ly}_{mn} = \frac{4}{\pi} t^2 \int d\omega \,\mathrm{Im}\left[\left(g^L_{mm02} - g^L_{mm01}\right)\left(g^R_{nn\uparrow\uparrow 21} + g^R_{nn\downarrow\downarrow 21}\right)\right] f(\omega). \tag{32}$$

The angle dependence apparently disappears, but is included in the spin-orbit terms of $g^R_{nn\uparrow\uparrow 21}$ and $g^R_{nn\downarrow\downarrow 21}$, which are proportional to $\sin 2\theta$, as mentioned earlier.

The torque $\boldsymbol{N}^{Ly}_{mn}$ given by Eq. (32) vanishes in the present one-dimensional model because $g^L_{mm02} = g^L_{mm01}$. However, the degeneracy of orbitals 1 and 2 may easily be lifted; for example, by lattice distortions, and $\boldsymbol{N}^{Ly}_{mn}$ remains to be nonzero. In more realistic models with two- and three-dimensional lattices and noncubic lattices, orbital degeneracy is naturally lifted. Therefore, the nonvanishing orbital torque is plausible in realistic NM/I/FM junctions. The nonvanishing orbital torque in the NM/I/FM junctions can be interpreted in the same manner as that given for Eq. (24): MA caused by the existence of the junction structure produces the orbital torque at the junction. The long-range character of MA [38] acting through the junction and the nondegeneracy of the orbital states are responsible to the flow of the orbital current.

Let us now compare the results for the spin and orbital currents/torques. The z component of the spin current vanishes in the limit of zero bias as seen in Eq. (19). However, all components of the orbital torque appear nonzero even in the zero-bias limit. The differences in the results can be attributed to the difference in the mathematical form of $\boldsymbol{\sigma}$ and $\boldsymbol{L}$: The former is the spinor operator, while the latter is the three-dimensional matrix operator. Different basis functions Y_{LM} might be used for OAM; however, the electronic states must be calculated using the basis functions, and the final expression of the current should be the same.

The longitudinal spin and orbital currents/torques studied in this work vanish when the entire system is paramagnetic. This feature is in strong contrast with the SHE and OHE studied in the paramagnetic metals. Dependence on the SOC also differs from each other [15]. For a further understanding for transverse and longitudinal spin and orbital currents/torques, more detailed analyses seem to be desirable [40].

C. Discussion

The calculated results were obtained under restricted conditions: the SAM and OAM are always collinear and their magnitude is unchanged in the rotated states (uniform rotation). Furthermore, the SOC was introduced at only the edge site of right electrode. Other effects such as lattice distortion, finite-temperature effect, etc., have been neglected. Discussions on these points are given below.

The assumption of the uniform rotation would be reasonable when the angles θ and φ are sufficiently small and the increase in the coupling energy between FM layers caused by the magnetization rotation is smaller than the spin-orbit energy. In this case the second-order perturbation may be effective; however, higher-order perturbations must be incorporated to include effects of mixing of SAM and OAM and of change in their magnitude under their rotation. Inclusion of SOC only at the edge site may neglect effects of the change in the electronic states caused by SOC on the other sites. Nevertheless, the qualitative feature of the spin and orbital torque could be obtained in the present study, because the edge sites are the most crucial part of the lattice to produce the torque/coupling at the interface of the junction [38]. We have ignored torque transfer to the lattice, which could be one of the important issues in future.

Now we estimate the order of magnitude of the orbital coupling and propose possible methods for observing the orbital coupling. As explained in Sec. II, coupling energy $E(\theta)$ is defined by $\int N(\theta)d\theta$ with a $\theta \to 0$ limit. From the expression of the torque in Eq. (27), the orbital coupling energy can be expressed as

$$E(0) \equiv E_{\mathrm{orb}} \sim t^2\xi^2 \int d\omega [g^R(\omega)]^4 f(\omega), \tag{33}$$

where the quartic term of the retarded GF originates from the second-order perturbation to SOC. Because the energy scale of $g^R(\omega)$ can be $1/W$ per atom, where W is the bandwidth and the integral provides additional energy W, $E_{\mathrm{orb}} \sim t^2\xi^2/W^3$ is obtained per atom. By considering $W \sim 5$ eV and $\xi \sim 0.1$ eV [15] and assuming $t \sim 10^{-3}$ eV, the magnitude of E_{orb} is 10^{-10} eV per atom. This value may be compared with the spin coupling energy E_{spin}. The calculated value of E_{spin} is approximately 3×10^{-6} eV/atom for the Co/Cu/Co trilayer with seven Cu atomic layers [33]. As expected, E_{orb} is significantly smaller than E_{spin} in a metallic junction. This difference is primarily due to the effects of the SOC and tunnel barrier. Additionally, the difference arises from the difference between orbital moment (m_{orb}) and spin moment (m_{spin}), because the orbital (spin) coupling energy must be proportional to the square of m_{orb} (m_{spin}). Recently, Sakamoto *et al.* [35] obtained $m_{\mathrm{orb}}/m_{\mathrm{spin}} \sim 0.04$ for Fe near the MgO/Fe interface using depth-resolved x-ray magnetic circular dichroism and first principles. Even when the latter effect is considered, E_{orb} may be smaller than E_{spin}. Therefore, enhancement of E_{orb} should be attempted to render orbital coupling observable. Among the ingredients listed above, control of hopping integral $\boldsymbol{t}$ by reducing the barrier thickness and/or barrier height is the most effective for this enhancement. Moreover, the SOC can be enhanced at edge sites of magnetic layers [38].

Nevertheless, the observation of orbital coupling may be nontrivial because spin coupling is also included in the entire coupling. Therefore, the orbital contributions should be carefully separated from the spin torque/coupling. Separation can be performed by noting that only spin torque vanishes for the NM/I/FM junctions. Furthermore, we must separate the contribution caused by the existence of the interface from that owing to the effects of the SOC itself. Such a separation can be realized by measuring several combinations of junction materials because SOC and interlayer hopping may contribute differently to the magnitude of the orbital torque. In addition, orbital torque/coupling acting on the OAM may cause relaxation in the direction OAM, which can be observed via ferromagnetic resonance for example, as reported in [18]. For quantitative comparison between experimental and theoretical results, it is desirable to formulate more explicit expressions for the orbital torque in systems with clear orbital moments.

IV. SUMMARY

This study formulated the longitudinal spin and orbital currents through tunnel junctions with SOC. We first derived a general form of the orbital currents at the interface using nonequilibrium GF formalism. Subsequently, the explicit formulas for the y and z components of the spin and orbital currents/torques are derived for the one-dimensional lattice model. We applied second-order perturbation to the hopping term in the insulator as well as to the SOC in the Hamiltonian. The coupling energy between OAMs (SAMs) at the interface was derived as the difference in the orbital (spin) currents at the junction interface.

The results of this study can be summarized as follows. The orbital torque is caused by SOC and relaxes through the junction interface as an orbital current, resulting in an orbital coupling between two magnetic layers. The orbital and the spin torques acting at the interface contain additional angle dependence owing to SOC in addition to the ordinary $\sin\theta$ term for the spin torque. The direction of the torque acting on OAM is determined by the SOC. Furthermore, the orbital torque may remain finite even for NM/I/FM junctions. The origin of the orbital torque at the junction has been attributed to MA caused by the junction structure, indicating the importance of the long-range character of MA and nondegeneracy of orbital states. Finally, the effects of finite voltage at the junction of the torque was clarified.

The magnitude of the orbital coupling energy was estimated, and methods to observe orbital torque/coupling were proposed. The difference between the longitudinal orbital (spin) current investigated in this study and the transverse current of OHE (SHE) was discussed; however, this remains a fundamental issue, and should be studied further in the future. The numerical calculations for more realistic models are also left for future research.

ACKNOWLEDGMENTS

This work was partially supported by CREST (Grant No. JPMJCR17J5) from Japan Science and Technology Agency (JST), the Initiative to Establish Next-Generation Novel Integrated Circuit Centers (X-NICS) (Grant No. JPJ011438) from Ministry of Education, Culture, Sports, Science and Technology (MEXT), and the Cooperative Research Project Program (Grant No. R03/B01) of Research Institute of Electrical Communication (RIEC), Tohoku University.

[1] S. Maekawa and T. Shinjo (eds.), *Spin Dependent Transport in Magnetic Nanostructures* (Taylor and Francis, New York, 2002).

[2] T. Shinjo (ed.), *Nanomagnetism and Spintronics* (Elsevier, Amsterdam, 2009).

[3] L. Berger, Emission of spin waves by a magnetic multilayer traversed by a current, Phys. Rev. B **54**, 9353 (1996).

[4] J. C. Slonczewski, Current-driven excitation of magnetic multilayers, J. Magn. Magn. Mater. **159**, L1 (1996).

[5] S. Murakami, N. Nagaosa, and S. C. Zhang, Dissipationless quantum spin current at room temperature, Science **301**, 1348 (2003).

[6] J. Sinova, D. Culcer, Q. Niu, N. A. Sinitsyn, T. Jungwirth, and A. H. MacDonald, Universal Intrinsic Spin Hall Effect, Phys. Rev. Lett. **92**, 126603 (2004).

[7] J. I. Inoue, G. E. W. Bauer, and L. W. Molenkamp, Suppression of the persistent spin Hall current by defect scattering, Phys. Rev. B **70**, 041303(R) (2004).

[8] V. M. Edelstein, Spin polarization of conduction electrons induced by electric current in two-dimensional asymmetric electron systems, Solid State Commun. **73**, 233 (1990).

[9] J. I. Inoue, G. E. W. Bauer, and L. W. Molenkamp, Diffuse transport and spin accumulation in a Rashba two-dimensional electron gas, Phys. Rev. B **67**, 033104 (2003).

[10] I. M. Miron, K. Garello, G. Gaudin, P.-J. Zermatten, M. V. Costache, S. Auffret, S. Bandiera, B. Rodmacq, A. Schuhl and R. Gambardella, Perpendicular switching of a single ferromagnetic layer induced by in-plane current injection, Nature (London) **476**, 189 (2011).

[11] L. Liu, C.-F. Pai, Y. Li, H. W. Tseng, D. C. Ralph, and R. A. Buhrman, Spin-torque switching with the giant spin Hall effect of tantalum, Science **336**, 555 (2012).

[12] P. M. Haney and M. D. Stiles, Current-Induced Torques in the Presence of Spin-Orbit Coupling, Phys. Rev. Lett. **105**, 126602 (2010).

[13] A. Manchon, J. Železný, I. M. Miron, T. Jungwirth, J. Sinova, A. Thiaville, K. Garello, and P. Gambardella, Current-induced spin-orbit torques in ferromagnetic and antiferromagnetic systems, Rev. Mod. Phys. **91**, 035004 (2019).

[14] H. Kontani, T. Tanaka, D. S. Hirashima, K. Yamada, and J. Inoue, Study of intrinsic spin and orbital Hall effects in Pt based on a (6*s*, 6*p*, 5*d*) tight-binding model, J. Phys. Soc. Jpn. **76**, 103702 (2007).

[15] T. Tanaka, H. Kontani, M. Naito, T. Naito, D. S. Hirashima, K. Yamada, and J. Inoue, Intrinsic spin Hall effect and orbital Hall effect in 4*d* and 5*d* transition metals, Phys. Rev. B **77**, 165117 (2008).

[16] H. Kontani, T. Tanaka, D. S. Hirashima, K. Yamada, and J. Inoue, Giant Intrinsic Spin and Orbital Hall Effects in Sr_2MO_4 (M = Ru, Rh, Mo), Phys. Rev. Lett. **100**, 096601 (2008).

[17] D. Go, D. Jo, C. Kim, and H.-W. Lee, Intrinsic Spin and Orbital Hall Effects form Orbital Texture, Phys. Rev. Lett. **121**, 086602 (2018).

[18] S. Ding, A. Ross, D. Go, L. Bakdrati, Z. Ren, F. Freimuth, S. Becker, F. Kammerbauer, J. Yang, G. Jakob, Y. Mokrousov, and M. Kläui, Harnessing Orbital-to-Spin Conversion of Interfacial Orbital Currents for Efficient Spin-Orbit Torques, Phys. Rev. Lett. **125**, 177201 (2020).

[19] S. Lee, M.-G. Kang, D. Go, D. Kim, J.-H. Kang, T. Lee, G.-H. Lee, J. Kang, N. J. Lee, Y. Mokrousov, S. Kim, K.-J. Kim, K.-J. Lee, and B.-G. Park, Efficient conversion of orbital Hall current to spin current for spin-orbit torque switching, Commun. Phys. **4**, 234 (2021).

[20] D. Go and H.-W. Lee, Orbital torque: Torque generation by orbital current injection, Phys. Rev. Res. **2**, 013177 (2020).

[21] D. Lee, D. Go, H.-J. Park, W. Jeong, H.-W. Ko, D. Yun, D. Jo, S. Lee, G. Go, J.-H. Oh, K.-J. Kim, B.-G. Park, B.-C. Min, H. C. Koo, H.-W. Lee, O. Lee, and K.-J. Lee, Orbital torque in magnetic bilayers, Nature Commun. **12**, 6710 (2021).

[22] A. Johansson, B. Gobel, J. Henk, M. Bibes, and I. Mertig, Spin and orbital Edelstein effects in a two-dimensional electron gas: Theory and application to $SrTiO_3$ interfaces, Phys. Rev. Res. **3**, 013275 (2021).

[23] S. Bhowal and S. Satpathy, Intrinsic orbital moment and prediction of a large orbital Hall effect in two-dimensional transition metal dichalcogenides, Phys. Rev. B **101**, 121112(R) (2020).

[24] I. Baek and H.-W. Lee, Negative intrinsic orbital Hall effect in group XIV materials, Phys. Rev. B **104**, 245204 (2021).

[25] Y.-G. Choi, D. Jo, K.-H. Ko, D. Go, K.-H. Kim, H. G. Park, C. Kim, B.-C. Min, G.-M. Choi, and H.-W. Lee, Observation of the orbital Hall effect in a light metal Ti, Nature **619**, 52 (2023).

[26] P. Grünberg, R. Schreiber, Y. Pang, M. B. Brodsky, and H. Sowers, Layered Magnetic Structures: Evidence for Antiferromagnetic Coupling of Fe Layers across Cr Interlayers, Phys. Rev. Lett. **57**, 2442 (1986).

[27] S. S. P. Parkin, N. More, and K. P. Roche, Oscillations in Exchange Coupling and Magnetoresistance in Metallic Superlattice Structures: Co/Ru, Co/Cr, and Fe/Cr, Phys. Rev. Lett. **64**, 2304 (1990).

[28] D. M. Edwards, J. Mathon, R. B. Muniz, and M. S. Phan, Oscillations of the Exchange in Magnetic Multilayers as an Analog of de Haas–van Alphen Effect, Phys. Rev. Lett. **67**, 493 (1991).

[29] P. Bruno and C. Chappert, Oscillatory Coupling between Ferromagnetic Layers Separated by a Nonmagnetic Metal Spacer, Phys. Rev. Lett. **67**, 1602 (1991).

[30] C. Caroli, R. Comberscot, P. Nozieres, and D. Saint-James, A direct calculation of the tunneling current: I, J. Phys. C **4**, 916 (1971).

[31] C. Caroli, R. Comberscot, P. Nozieres, and D. Saint-James, A direct calculation of the tunneling current: IV, Electron-phonon interaction effects, J. Phys. C **5**, 21 (1972).

[32] D. M. Edwards, A. M. Robinson, and J. Mathon, The torque method for exchange coupling in magnetic trilayers, J. Magn. Magn. Mater. **140–144**, 517 (1995).

[33] J. Mathon, M. Villeret, R. B. Muniz, J. d'Albuquerque e Castro, and D. M. Edwards, Quantum Well Theory of the Exchange Coupling in Co/Cu/Co(001), Phys. Rev. Lett. **74**, 3696 (1995).

[34] D. M. Edwards, F. Federici, J. Mathon, and A. Umerski, Self-consistent theory of current-induced switching of magnetization, Phys. Rev. B **71**, 054407 (2005).

[35] S. Sakamoto, M. Tsujikawa, M. Shirai, K. Amemiya, and S. Miwa, Electron correlation enhances orbital polarization at a ferromagnetic metal/insulator interface: Depth-resolved x-ray magnetic circular dichroism and first-principles study, ACS Appl. Electron. Mater. **4**, 1794 (2022).

[36] J. I. Inoue, Analytical expression for the spin-transfer torque in a magnetic junction with a ferromagnetic insulator, Phys. Rev. B **84**, 180402(R) (2011).

[37] D.-S. Wang, R. Wu, and A. J. Freeman, Magnetocrystalline anisotropy of Co-Pd interfaces, Phys. Rev. B **48**, 15886 (1993).

[38] J. Inoue, Real-space representation of uniaxial magnetic anisotropy of ferromagnetic metals with non-periodic structures, J. Phys. D: Appl. Phys. **48**, 445005 (2015).

[39] V. Heine, Electronic structure from point of view of the local atomic environment, in *Solid State Physics*, edited by H. Ehrenreich, F. Seitz, and D. Turnbull (Academic Press, New York, 1980), Vol. 35, p. 1.

[40] M. Tsujikawa *et al.*, A first-principles study on OHE (unpublished).